

Keywords: mammography, transfer learning, computer vision, image processing

Muayed S AL-HUSEINY [0000-0003-3192-0232]*, *Ahmed S SAJIT* [0000-0002-1894-9033]**

BREAST CANCER CAD SYSTEM BY USING TRANSFER LEARNING AND ENHANCED ROI

Abstract

Computer systems are being employed in specialized professions such as medical diagnosis to alleviate some of the costs and to improve dependability and scalability. This paper implements a computer aided breast cancer diagnosis system. It utilizes the publicly available mini MIAS mammography image dataset. Images are preprocessed to clean isolate breast tissue region. Extracted regions are used to adjust and verify a pretrained convolutional deep neural network, the GoogLeNet. The implemented model shows good performance results compared to other published works with accuracy of 86.6%, sensitivity of 75% and specificity of 88.9%.

1. INTRODUCTION

Breast cancer is one of the most frequently occurring types of cancers (Batra, Sekhar & Radha, 2020). It is reported that in the year 2018 alone more than two million new cases were diagnosed (Breast Cancer Facts and Statistics, 2018). A study conducted by Cancer research UK showed that almost all women diagnosed with breast cancer at earlier stages are most likely to live for at least 5 years after their diagnosis compared to only 15% of those diagnosed at later stages (Survival, 2018). A recent report sponsored by Breast Cancer Care revealed that more than 40% of UK National Health Service (NHS) trusts lack the qualified specialist nurses to manage breast cancer (Written evidence (RTR0073), n.d.). Further, it is reported that the survival rates of cases of breast cancer in developing countries is under 40% with the main factor for such low rates being the scarcity of early diagnosis programs as well as the lack of specialized facilities and trained staff (Breast cancer: prevention and control, 2008). These findings together with the fact that this type of cancer is invasive necessitates particular attentiveness of medical and technological communities alike (Batra et al., 2020). This is an important area of research because during conventional examination by a radiologist, non-cancerous lesions can be misclassified as a cancer (false-positive), while malignancies may be missed (false-negative) resulting in radiologists failing to detect between 10% and 30% of breast cancers cases. Computer aided diagnosis (CAD) is aimed to speed up and enhance the diagnosis process via assisting specialists in the detection and classification of the breast cancer by deploying scalable computerized diagnostic tools,

* Wasit University, Department of Electrical Engineering, Iraq, malhuseiny@uowasit.edu.iq

** Wasit University, College of Engineering, Iraq, aalhuseiny@uowasity.edu.iq

hence, restricting the occurrence of human related shortcomings (AL-Huseiny & Sajit, 2021; Batra et al., 2020; Jalalian et al., 2013; Tan, Sim & Ting, 2017). The introduction of computerized approaches into medical procedures is highly reliant on the sensing mechanisms. Depending on the particular clinical condition and region in the human body, medical doctors utilize among a pool of diagnostic tools starting from physical inspection, patient history, lab tests and extending to sophisticated imaging procedures such as x-ray, ultrasonography, CT scans, MRI, mammography and etc. Successful exploitation of modern powerful computation in CAD is closely related to the development of computer algorithms to work with each of these diagnostic tools, particularly, different imaging modalities (Yadav & Yadav, 2020). Mammography is one of the most widely used method in the diagnosis of breast cancer. It is a relatively inexpensive screening procedure that usually takes between 10 and 15 minutes to perform (Davis, 2021). In most computer imaging procedures, CAD systems are constituted of four parts: (a) preprocessing, (b) detection of regions of interest (ROI), (c) feature selection/extraction, and (d) classification (Jalalian et al., 2013). The reliability of conventional classification methods resides in the implementation of a suitable data representation. Much of the efforts in this regard are dedicated to the identification of discriminative traits, a difficult and time-demanding operation that requires the knowledge of domain experts (Spanhol et al., 2016a). Many CAD approaches employ a combination of hand-designed heuristic features with mathematical descriptor features (Zeiler, Taylor & Fergus, 2011). An alternative path is to derive features automatically from training images (Lazebnik, Schmid & Ponce, 2006). Recent advancements allowed machine learning/computer vision tasks to perform feature learning feasibly. Convolutional neural networks (CNN) which perform local connectivity pattern among neurons of successive layers can characterize spatial locality of input features yielding highly dependable feature extraction. Combined with the inherent powerful generalization capability of deep neural networks, these together are projected to form a strong CAD system candidate for breast cancer (Batra et al., 2020).

1.1. Literature Review

In previous related studies, the authors in (Batra et al., 2020) used preprocessing to enhance input images and followed that by image segmentation to extract strips of the malignant tissue. These are then fused with the original images to train their 8 layers custom-built CNN. They also studied the trade-off between accuracy and training in various execution environment such as Tensorflow and Matlab. The authors in (Jamieson, Drukker & Giger, 2012) modified the Adaptive Deconvolutional Networks (Zeiler, Taylor & Fergus, 2011) into multiple layers of representation to learn two datasets of breast image data: full field digital mammography (FFDM) and ultrasound sets. They employed Spatial Pyramid Matching to the inferred feature maps and used linear support vector machine for classification to achieve moderate performance. CNNs are also used in detection and analysis using histopathology images, the authors in (Zainudin, Shamsuddin & Hasan, 2021) proposed four types of deep layer CNN architecture which are called 6-layer CNN, 13-layer CNN, 17-layer CNN and 19-layer CNN, respectively, to detect malignant cells (mitosis) in breast tissue by using histopathology image and to compare the performance of different layered implementations. Spanhol et al (Spanhol et al., 2016a) also implemented a deep learning approach to classify breast cancer histopathological images taken from the publicly

available BreKHis dataset (Spanhol et al., 2016b). They suggested a method to extract image patches to train the CNN and then combined these patches with the original images for final classification. The study employs transfer learning and also combines different CNNs by using simple fusion rules with some reported improvement accuracy. Masud et al (Masud, Eldin Rashed & Hossain, 2020) in their research also consider transfer learning. They fine-tuned eight different pre-trained models as well as a proposed shallow convolutional neural network to compare the performance of these models in classifying breast cancers on two merged ultrasound datasets. Noise was removed by applying morphological operations to extract the ROIs. The achieved results show that the performance of the proposed CNN outperforms that of the pre trained models. Arevalo et al. (Arevalo et al., 2016) suggested a new representation learning framework for the diagnosis of breast cancer in mammograms which merges deep learning with the automatic learning of features. They built a new biopsy proven dataset and followed a hybrid approach, hence, CNNs are used to learn the features in a supervised setting. Petersen et al (Petersen et al., 2014) implemented a convolutional sparse autoencoder (CSAE) method which extracts descriptive features from unlabeled mammograms taken from the Dutch biennial breast screening program dataset (Otten et al., 2005). The learned features are used to train a simple classifier which performs tissue segmentation, scoring of percentage mammographic density (PMD), and scoring of mammographic texture (MT). The authors in (Tan, Sim & Ting, 2017) employed Google's TensorFlow to develop their classifier on mini-MIAS mammogram dataset. They used preprocessing to crop abnormality tissues to 48 x 48 and then fed those features to CNN classifier as training source. Authors in (Charan, Khan & Khurshid, 2018) suggested a transfer learning model based on GoogleNet and AlexNet pre-trained models, they also utilized preprocessing techniques. Their proposed model is applied to mammograms with segmented cancer regions. The authors claim that the model achieves improved performance over human involved methods.

The research problem addressed in this paper is to design a learning based computer aided breast cancer diagnosis system. This is pursued building on previous efforts by implementing CAD system where preprocessing is used to rid input images of markings, edges, and unrelated body tissues. ROI containing only breast region is then segmented and used to adjust and test a pretrained deep CNN. the rest of this paper includes, in section two the material and methods used, the results in section three and finally the conclusions in section four.

2. MATERIALS AND METHODOLOGY

The proposed framework consists of a set of pre-processing steps, followed by the setup of a machine learning model. The model is trained and validated by using mammographic image dataset. The various stages of the framework are presented subsequently.

2.1. MIAS Dataset

This digital dataset was generated by the (Mammographic Image Analysis Society-MIAS (Suckling et al., 1994) which is a research body focused on the development and understanding of mammograms. Images produced via the (UK National Breast Screening Program) were used for the generation of the dataset after digitization of the original scans.

The digital images are utilized in a 50-micron pixel edge by using a Joyce-Loebl microdensitometer at 8-bit resolution per pixel (see Fig. 1-a and Fig. 2-a). The dataset includes a total of 322 digital images (161 patients) along with expert radiologist annotations specifying the regions of detected abnormalities. The dataset is publicly accessible through the Pilot European Image Processing Archive (PEIPA) at the University of Essex (Grgic et al., 2021). The provided information describing the dataset includes:

1. The type of the background tissue: fatty, fatty-glandular and dense-glandular.
2. The detected abnormality: calcification; circumscribed masses, etc.
3. The degree of abnormality: benign and malignant.
4. The coordinates of the abnormality on the digitized image.
5. The radii of the circles surrounding the lesions.

The image files in the dataset are organized in consecutive odd/even numbered pairs representing respectively the right and left mammograms of individual patients. The images were normalized to the center of the 1024x1024 grid with origin represented by the lower left element of the grid.

2.2. Pre-processing

In most classification applications, preprocessing plays a crucial role in exposing and magnifying discriminatory features. It is used in this research to perform two functions: to rid unnecessary markings and human tissues, and to normalize the appearance of all images. As such the resulting images will be a relatively clean centered region of interest (ROI) with normalized size and intensity for all files of the used dataset. The stages of preprocessing are summarized:

Gabor filter (Aach, Kaup & Mester, 1995) is used to characterize differently textured tissue parts. This will help remove unrelated markings and structures. Gabor filters are bandpass filters frequently used in image processing applications, particularly, in dealing with human tissues as texture is a more discriminant trait than other features such as shape, brightness or etc. Eq. (1) gives the response of Gabor mask to an input image $X(r, c)$:

$$G_{r c} = \exp\left(-\frac{\hat{r}^2 + \gamma^2 \hat{c}^2}{2\sigma^2}\right) \cos\left(2\pi \frac{\hat{r}}{\lambda} + \psi\right) \quad (1)$$

where $\hat{r} = r \cos \theta + c \sin \theta$, and, $\hat{c} = r \sin \theta + c \cos \theta$ of $X(r, c)$. Filter parameters are: λ represents the wavelength, θ is the angle of the normal to the wave of a Gabor function, ψ is the phase shift, σ is the Gaussian standard deviation and γ is the aspect ratio (AL-Huseiny & Sajit, 2021; Gabor filter, n.d.). The values of these parameters are tuned to achieve best results with respect to the input images in terms of emphasizing unwanted structures to be eliminated by later stages of preprocessing. the output of Gabor filter is thresholded as shown in Fig. 1-b and Fig. 2-b.

Morphological operations: after Gabor filter, the images are treated with morphological operators with carefully selected structuring element. This helps remove small and densely perforated regions after texture analysis, including markings and muscle tissue as depicted in the examples of Fig. 1-c and Fig. 2-c. morphological operation is given in Eq. (2):

$$G_{Mrph} = Morph_{sel}(G) \quad (2)$$

where G_{Mrph} is the output of morphological operator $Morph$ performing under the structuring element sel .

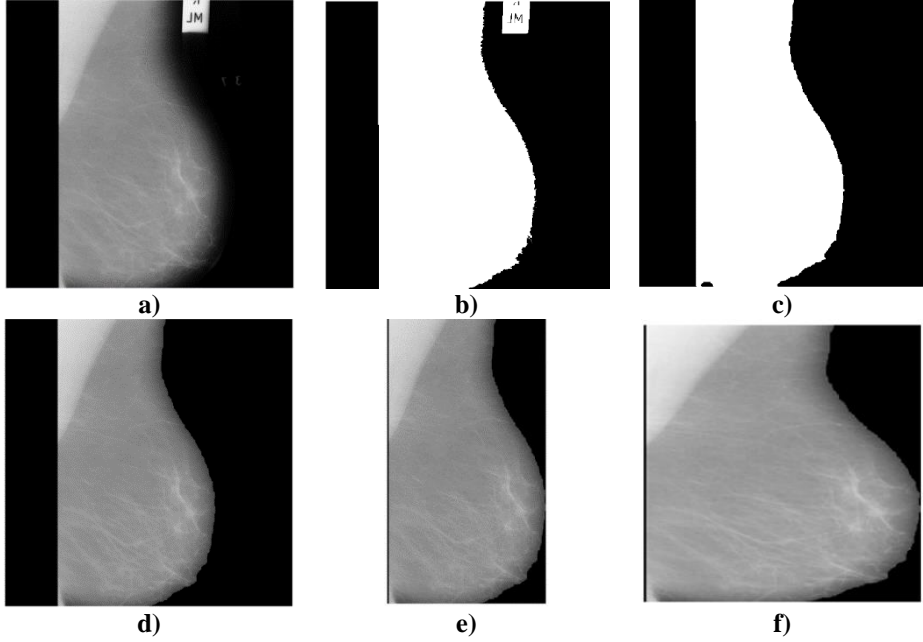


Fig. 1. Stages of preprocessing – example 1: a) input image, b) texture analysis followed by thresholding, c) morphological operation and region selection, d) masking of original image, e) cropping to ROI, and f) size and intensity normalization

Region selection: in cases where more than one region is left after morphological operations, the region with the largest area is preserved while other regions are omitted from the binary image forming a mask G_{Msk} for the desired ROI.

Masking: input images are multiplied by their respective masks to extract their ROIs as given by Eq. (3). This is shown in Fig. 1-d and Fig. 2-d.

$$X_{ROI} = \sum_{r,c} X(r,c) * G_{Msk}(r,c) \quad (3)$$

Cropping: masked images are then cropped to the boundaries of the extracted region to give X_{Crd} . The results of this stage can be seen in Fig. 1-e and Fig. 2-e

Normalization: this step includes both size and intensity normalization, thus, each cropped image of ROI is scaled to 224X224 pixels image X_{Scl} . Scaled images are then intensity normalized according to Eq. (4) (Gonzalez & Woods, 2006):

$$X_{Nrm} = (X_{Scl} - Min) \frac{newMax - newMin}{Max - Min} + newMin \quad (4)$$

where X_{Scl} and X_{Nrm} are scaled and output normalized images respectively, Min and Max are minimum and maximum values of the input scaled image, $newMin$ and $newMax$ are

the desired minimum and maximum values of the normalized image, in this research these values are set to 0 and 1 respectively. The output of this stage is presented in the examples of Fig. 1-f and Fig. 2-f.

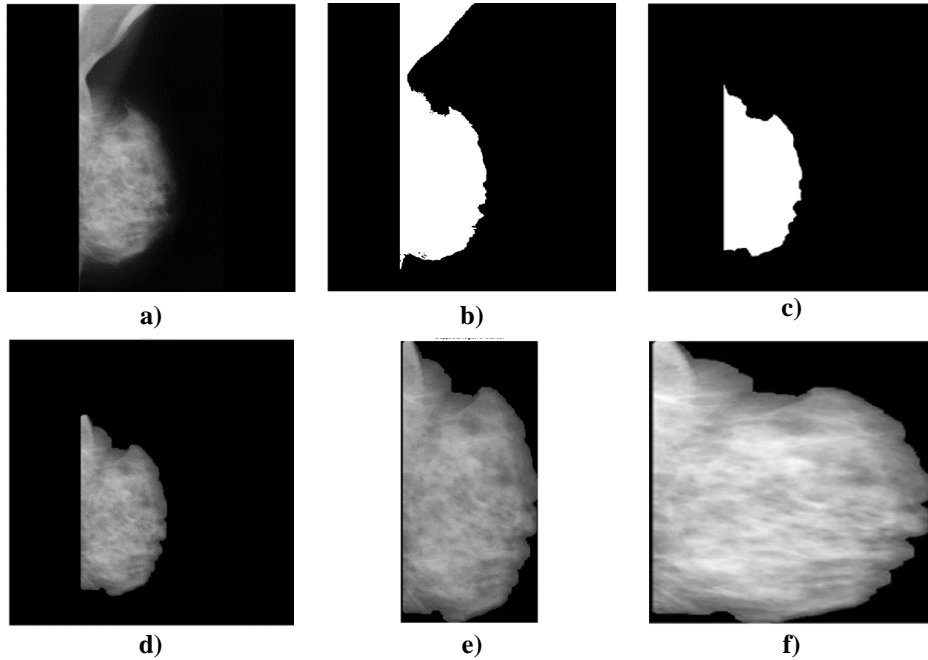


Fig. 2. Stages of preprocessing – example 2: a) input image, b) texture analysis followed by thresholding, c) morphological operation and region selection, d) masking of original image, e) cropping to ROI, and f) size and intensity normalization

2.3. Transfer learning with GoogLeNet

Transfer learning involves the use of previously developed computer models to learn patterns of new data different from that used in the development of these models (AL-Huseiny & Sajit, 2021). This approach is useful particularly when the available resources such as data and computing power are limited. The attractiveness of such strategy should not distract from the fact that not all trained models are capable of learning previously unseen data. Thus, the process involves some sort of tuning to parts of the transferred models to ensure that there is a compatibility in terms of data types as well as expected classes. In Fig. 3 it is noticed that early layers are largely kept unchanged due to the fact that these layers are activated on low level features and this is the type of knowledge desirable to be transferred to the new domain. Subsequent and last layers are obviously replaced and trained with the new data (domain), the reason is that these layers model data specific attributes, as such, they are activated by high level features (AL-Huseiny, Abbas & Sajit, 2020; AL-Huseiny & Sajit, 2021; Al-Yasriy et al., 2020). The use of transfer learning strategy significantly diminishes training time as large parts of the network are at or near convergence.

Convolutional neural networks (CNNs) are a category of deep NNs widely utilized in the analysis of images and videos. These models are characterized by being shift/space invariant in the sense that their convolution filters which slide along input features use shared-weight architecture. This configuration gives translation equivariant responses commonly defined as feature maps (Convolutional neural network, n.d.; Zhang, 1990).

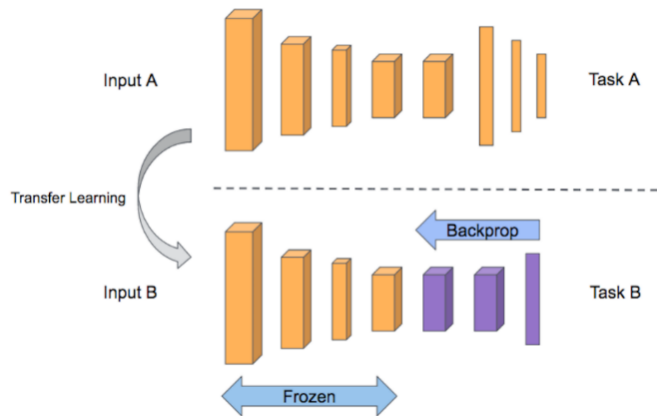


Fig. 3. The concept of transfer learning shown in terms of model layers – only learnable layers are readjusted (Malgonde, 2021)

GoogLeNet is a Convolutional NN developed by Szegedy et al (Szegedy et al., 2015) for the ImageNet challenge (Russakovsky et al., 2015). This challenge involves the development of high feature representations by millions of images of ordinary objects collected in a huge dataset. The network architecture is formed mainly of stacking of Inception modules as shown in Fig 4. The layers of this deep CNN are listed in Table 1. As a standard approach in computer vision with deep learning, this CNN classifies input images into one of the learned classes and produces a value representing the level of confidence of the output. The configuration of this CNN ensures that it has 12 times less parameters than Alexnet (Santos, 2019). The structure of GoogLeNet constitutes 22 layers. Notably, 9 prominently important constructions called the inception modules.

Inception modules depicted in Fig. 5 employ learnable filters ranging in size from (1×1) to (5×5) and are specialized in emphasizing various level features simultaneously (Szegedy et al., 2015). These structures act on analyzing the correlation statistics coming out of the activations of preceding layers. Correlated activations are clustered together in one vector (Tripathy, 2016). This configuration is well suited for computer vision applications where higher correlations occur in local neighborhoods, hence, the use of 1×1 filters. As for general features spread across larger neighborhoods, larger filters will capture their correlations.

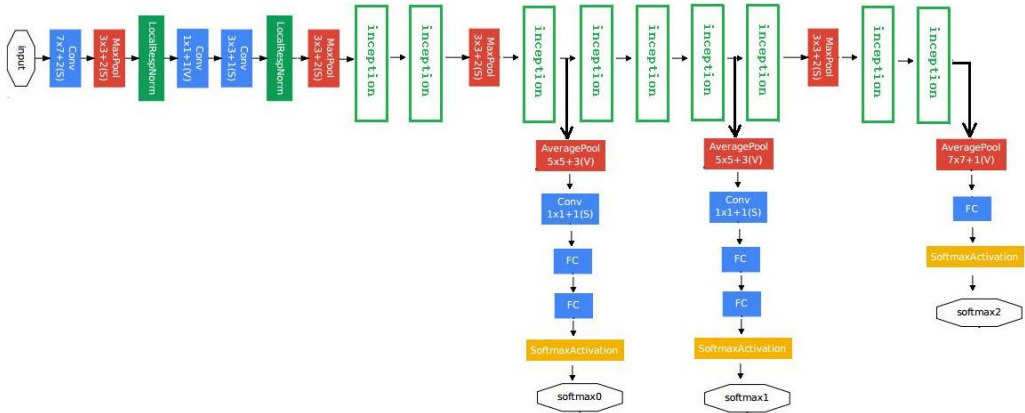


Fig 4: The architecture of GoogLeNet, inception modules are shown as blocks (Deep Learning Network Part Three: GoogLeNet Series, n.d.; Melli, 2021)

Tab. 1. The Layers of The GoogLeNet CNN

	Name	Count	Activation
1.	Input layer	1	/
2.	Convolutional layers	3	/
3.	Max-pooling layers	3	/
4.	Inception module layers;	9	/
5.	Average pooling layers	2	/
6.	Normalization layers	2	/
7.	Dropout layer	1	/
8.	Fully connected layer	1	ReLU
9.	Output layer	1	Softmax

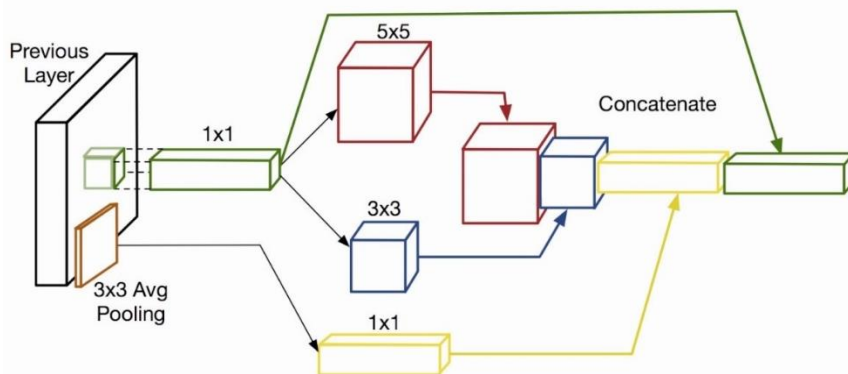


Fig. 5. The organization of filters within the inception module (Szegedy et al., 2015; Tripathy, 2016)

2.4. Experimental

The current study employs the digitized images of the mini MIAS mammographic slides (Suckling et al., 1994). Depending on the specialists' diagnosis, this sample divides its cases into three categories: Normal (NRM), Benign (BGN) and Malignant (MLG). Images are initially prepared as detailed in Sec 2.2 to extract the ROI. The sample is then grouped into two sets for training and testing at the ratio of 70:30. The larger set is used to train the transferred GoogLeNet model and adjust its learnable weights. The second set is used to test the performance of the learned model. In this setting, the loss3 classifier (fully connected layer) and the output (classification) layers are replaced and fine-tuned by using the training data to accommodate data specific features and to produce the desired number of classes respectively.



Results	
Validation accuracy:	86.60%
Training finished:	Reached final iteration
Training Time	
Start time:	27-May-2021 06:55:57
Elapsed time:	56 min 20 sec
Training Cycle	
Epoch:	30 of 30
Iteration:	2160 of 2160
Iterations per epoch:	72
Maximum iterations:	2160
Validation	
Frequency:	72 iterations
Other Information	
Hardware resource:	Single CPU
Learning rate schedule:	Constant
Learning rate:	3e-05

Fig. 6. MATLAB user interface showing the parameters used in the training/testing of the deep neural network

For learning the model, the number of epochs was set to 30 with stochastic gradient descent (SGD) learning strategy. The learning rate was set to 3×10^{-5} except for the last layers which was at 3×10^{-4} , these values were chosen empirically. In order to assure better learning images were shuffled at the start of the epoch. Further, and avoid overfitting these images were augmented by using random scaling, translation and rotation. The model was implemented by using MATLAB® R2020b deep learning toolbox on a dual-core Intel Core i5 MacBook pro machine clocked at 2.5 GHz with 16 GB DDR3 RAM. The algorithm parameters were adjusted to the values listed in Fig. 6.

3. DATA ANALYSIS AND INTERPRETATION

The transfer learning approach employed in this research to use a pretrained deep neural network, the GoogLeNet was used to classify the mammograph images of the mini MIAS breast cancer dataset. The results show that the transfer learned model has achieved an accuracy of 86.6% for the test sample. In Fig. 7 the accuracy and the loss over the course of training and testing over 2160 iterations is shown. It is obvious that the algorithm begins settling after 1100 iterations. In the graphs of Fig. 7 continuous ripple is observed in the accuracy as well as the loss, this can be referred to the presence of noise and non-uniform imaging conditions common in real world data as well as the augmentation deployed to overcome overfitting.

A group of four randomly selected classified images is shown in Fig 8. The figure also provides the probability of the generated class for each image. It is evident that the algorithm in some cases is making guesses as would be the case with specialists. However, the majority of classifications is performed with high degree of confidence. The trained model also scores sensitivity of 75% and specificity of 88.9%, further detailed outcomes are presented in the confusion matrix of Tab. 1.

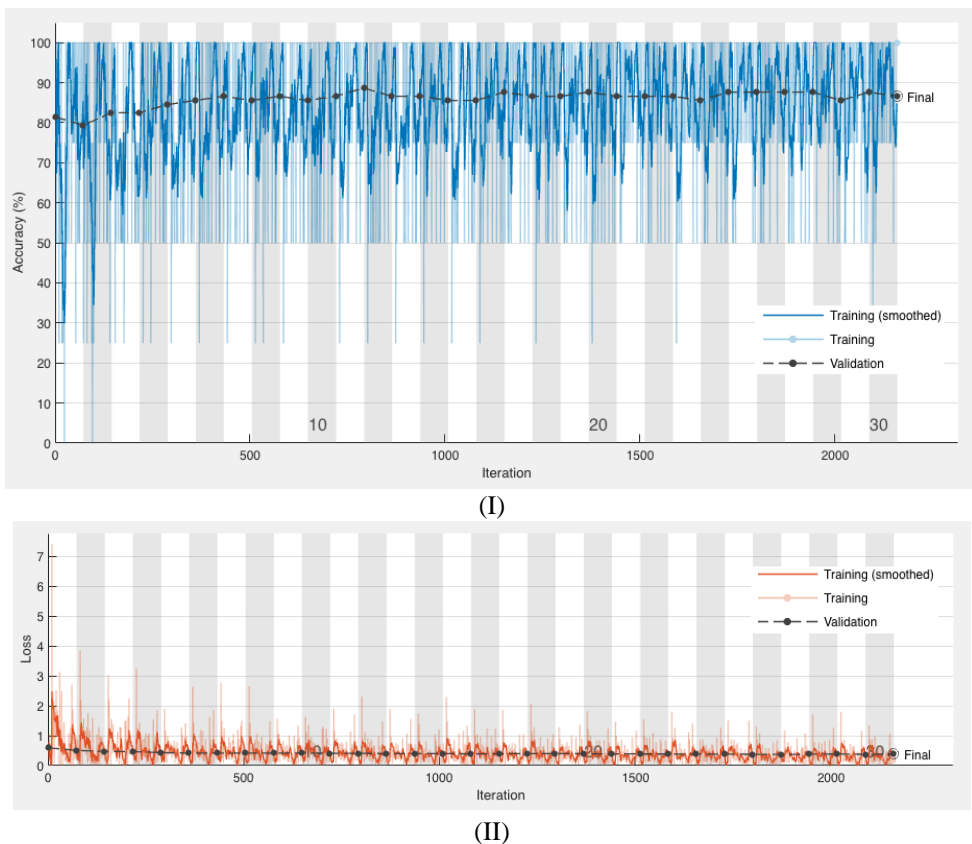


Fig. 7. The outcomes of the training/testing of the proposed transfer learning model over 30 epochs and 2160 iterations in terms of (I) accuracy, (I)loss

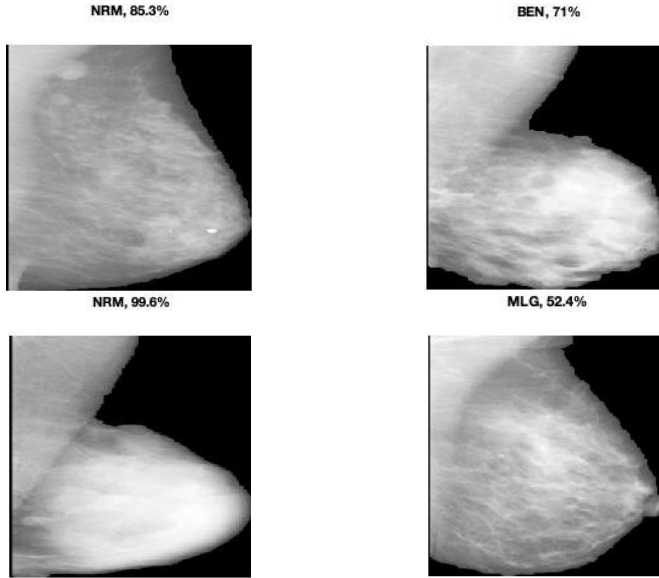


Fig 8: Examples of classified mammograph images selected at random, shown with the classification labels are the probabilities of the generated classes

The outcomes of the proposed implementation are measured against other related models mentioned in the literature. Tab. 3 provides comparison figures for the proposed system against those models, in which it shows that this work scored higher accuracy, and also, better specificity (where values were provided), which indicates an improved true negative and false positive rates. Sensitivity was slightly below that of other methods which refers to higher false negative cases produced by this approach compared to the other reported methods. Despite being better on other metrics, this aspect needs to be looked into and improved perhaps by using larger datasets or merging multiple datasets together to help the model learn deeper features in order to be more discriminative.

Tab. 2. Confusion Matrix

Confusion matrix		Predicted class	
		Non-malignant (positive)	Malignant (negative)
Actual class	Non-malignant	TP = 12	FN = 4
	Malignant	FP = 9	TN = 72

Tab. 3. Comparison of methods

Method	Dataset	Accuracy	Sensitivity	Specificity	Time
Batra (Batra, Sekhar & Radha, 2020)	mini MIAS	84.02%	/	/	45 minutes
BCDCNN (Tan, Sim & Ting, 2017)	mini MIAS	71%	82.68%	82.73%	/
Spanhol (Spanhol et al., 2016a)	BreaKHis	84%	/	/	/
Charan (Charan, Khan & Khurshid, 2018)	MIAS	65%	/	/	/
Zainudin (Zainudin, Shamsuddin & Hasan, 2021)	MITOS-ATYPHIA	84.49 %	80.55 %	/	/
Proposed	mini MIAS	86.6%	75%	88.9%	56 minutes

4. CONCLUSION

In this paper a computer aided diagnosis system for breast cancer is presented which employs a learning algorithm to model the data of publicly published mammographic images, the mini MIAS dataset. The images were initially preprocessed to clean and extract breast tissue only ROI and remove markings and clutter. They are then size and brightness normalized. The treated dataset was then augmented to compensate for the limited size of the sample. The set is then fed to the GoogLeNet CNN in a transfer learning approach to save training time and reuse derived features. Initial and final layers of the CNN were replaced to accommodate input data and the desired classes. This setting produced an accuracy of 86.6% which is better than those of the methods reported previously. Furthermore, this approach is easy to setup and modify. Therefore, compared to human experts it is scalable, reportedly more stable and less prone to subjective and circumstantial influences.

REFERENCES

- Aach, T., Kaup, A., & Mester, R. (1995). On texture analysis: Local energy transforms versus quadrature filters. *Signal Processing*, 45(2), 173-181. [https://doi.org/10.1016/0165-1684\(95\)00049-J](https://doi.org/10.1016/0165-1684(95)00049-J)
- AL-Huseiny, M. S., Abbas, N. K., & Sajit, A. S. (2020). Diagnosis of arrhythmia based on ECG analysis using CNN. *Bulletin of Electrical Engineering and Informatics*, 9(3), 988-995. <https://doi.org/10.11591/eei.v9i3.2172>
- AL-Huseiny, M. S., & Sajit, A. S. (2021). Transfer learning with GoogLeNet for detection of lung cancer. *Indonesian Journal of Electrical Engineering and Computer Science*, 22(2), 1078-1086. <http://doi.org/10.11591/ijeecs.v22.i2.pp1078-1086>
- Al-Yasriy, H. F., Al-Husieny, M. S., Mohsen, F. Y., Khalil, E. A., & Hassan, Z. S. (2020). Diagnosis of lung cancer based on CT scans using CNN. *IOP Conference Series: Materials Science and Engineering*, 928, 022035. <https://doi.org/10.1088/1757-899x/928/2/022035>
- Arevalo, J., González, F. A., Ramos-Pollán, R., Oliveira, J. L., & Guevara Lopez, M. A. (2016). Representation learning for mammography mass lesion classification with convolutional neural networks. *Computer Methods and Programs in Biomedicine*, 127, 248-257. <https://doi.org/10.1016/j.cmpb.2015.12.014>
- Batra, K., Sekhar, S., & Radha, R. (2020). Breast cancer detection using CNN on mammogram images. *Computational Vision and Bio-Inspired Computing* (pp. vol 1108). Springer. https://doi.org/10.1007/978-3-030-37218-7_80
- Breast Cancer Facts and Statistics. (2018). Retrieved June 12, 2021 from <https://www.breastcancer.org/facts-statistics>
- Breast cancer: prevention and control. (2008). World Health Organisation. <https://www.who.int/cancer/detection/breastcancer/en/index1.html#:~:text=Breast%20cancer%0survival%20rates%20vary,et%20al.%2C%202008>
- Charan, S., Khan, M. J., & Khurshid, K. (2018). Breast cancer detection in mammograms using convolutional neural network. *2018 International Conference on Computing, Mathematics and Engineering Technologies (iCoMET)* (pp. 1-5). IEEE. <https://doi.org/10.1109/ICOMET.2018.8346384>
- Convolutional neural network. (n.d.). *Wikipedia* Retrieved June 21, 2022 from https://en.wikipedia.org/w/index.php?title=Convolutional_neural_network&oldid=1029918158
- Davis, L. E. (n.d.). *What Is a Mammogram?* Retrieved June 20, 2021 from <https://www.verywellhealth.com/mammogram-what-to-expect-430283>
- Deep Learning Network Part Three: GoogLeNet Series*. (n.d.). Retrieved June 15, 2021 from <https://www.programmingsought.com/article/85103454206/>
- Gabor filter. (n.d.). *Wikipedia*. Retrieved June 21, 2022 from https://en.wikipedia.org/w/index.php?title=Gabor_filter&oldid=993157632
- Gonzalez, R. C., & Woods, R. E. (2006). *Digital Image Processing (3rd Edition)*. Prentice-Hall, Inc.
- Grgic, M., Delac, K., Bozek, J., & Rangayyan, R. M. (2021). *Mammographic image analysis homepage*. Video Communications Laboratory (VCL), Faculty of Electrical Engineering and Computing, University of Zagreb, Croatia.

- Jalalian, A., Mashohor, S. B., Mahmud, H. R., Saripan, M. I., Ramli, A. R., & Karasfi, B. (2013). Computer-aided detection/diagnosis of breast cancer in mammography and ultrasound: a review. *Clinical Imaging*, 37(3), 420-426. <https://doi.org/10.1016/j.clinimag.2012.09.024>
- Jamieson, A. R., Drukker, K., & Giger, M. L. (2012). Breast image feature learning with adaptive deconvolutional networks. *Proc. SPIE 8315, Medical Imaging 2012: Computer-Aided Diagnosis* (no. 831506). <https://doi.org/10.1117/12.910710>
- Lazebnik, S., Schmid, C., & Ponce, J. (2006). Beyond Bags of features: spatial pyramid matching for recognizing natural scene categories. *2006 IEEE Computer Society Conference on Computer Vision and Pattern Recognition (CVPR'06)* (pp. 2169-2178). IEEE. <https://doi.org/10.1109/CVPR.2006.68>
- Malgonde, S. (2021). *Transfer learning using Tensorflow*. <https://medium.com/@subodh.malgonde/transfer-learning-using-tensorflow-52a4f6bcde3e>
- Masud, M., Eldin Rashed, A. E., & Hossain, M. S. (2020). Convolutional neural network-based models for diagnosis of breast cancer. *Neural Computing and Applications*. Springer. <https://doi.org/10.1007/s00521-020-05394-5>
- Melli, G. (2021). *GoogLeNet*. <https://www.gabormelli.com/RKB/GoogLeNet>
- Otten, J. D. M., Karssemeijer, N., Hendriks, J. H. C. L., Groenewoud, J. H., Fracheboud, J., Verbeek, A. L. M., de Koning, H. J., & Holland, R. (2005). Effect of recall rate on earlier screen detection of breast cancers based on the dutch performance indicators. *JNCI: Journal of the National Cancer Institute*, 97(10), 748–754. <https://doi.org/https://10.1093/jnci/dji131>
- Petersen, K., Nielsen, M., Diao, P., Karssemeijer, N., & Lillholm, M. (2014). Breast tissue segmentation and mammographic risk scoring using deep learning. *Breast Imaging. IWDMM 2014. Lecture Notes in Computer Science* (vol 8539). Springer. https://doi.org/10.1007/978-3-319-07887-8_13
- Russakovsky, O., Deng, J., Su, H., Krause, J., Satheesh, S., Ma, S., Huang, Z., Karpathy, A., Khosla, A., Bernstein, M., Berg, A. C., & Fei-Fei, L. (2015). ImageNet large scale visual recognition challenge. *International Journal of Computer Vision*, 115(3), 211-252. <https://doi.org/10.1007/s11263-015-0816-y>
- Santos, L. (2019). *Artificial Intelligence*. GitBook.
- Spanhol, F. A., Oliveira, L. S., Petitjean, C., & Heutte, L. (2016a). Breast cancer histopathological image classification using Convolutional Neural Networks. *2016 International Joint Conference on Neural Networks (IJCNN)* (pp. 2560-2567). IEEE. <https://doi.org/10.0.4.85/IJCNN.2016.7727519>
- Spanhol, F. A., Oliveira, L. S., Petitjean, C., & Heutte, L. (2016b). A Dataset for Breast Cancer Histopathological Image Classification. *IEEE Transactions on Biomedical Engineering (TBME)*, 63(7), 1455–1462.
- Suckling, J., Astley, S., Betal, D., Cerneaz, N., Dance, D. R., Kok, S.-L., Parker, J., Ricketts, I., Savage, J., Stamatakis, E., & Taylor, P. (1994). *The Mammographic Image Analysis Society Digital Mammogram Database Excerpta Medica*. International Congress Series.
- Survival. (n.d.). Retrieved August 20, 2022 from <https://www.cancerresearchuk.org/about-cancer/breast-cancer/survival>
- Szegedy, C., Wei, L., Yangqing, J., Sermanet, P., Reed, S., Anguelov, D., Erhan, D., Vanhoucke, V., & Rabinovich, A. (2015). Going deeper with convolutions. *2015 IEEE Conference on Computer Vision and Pattern Recognition (CVPR)* (pp. 1–9). IEEE. <https://doi.org/10.1109/CVPR.2015.7298594>
- Tan, Y. J., Sim, K. S., & Ting, F. F. (2017). Breast cancer detection using convolutional neural networks for mammogram imaging system. *2017 International Conference on Robotics, Automation and Sciences (ICORAS)* (pp. 1–5). IEEE. <https://doi.org/10.1109/ICORAS.2017.8308076>
- Tripathy, A. (2016). *GoogLeNet Insights* slideshare.net. https://www.youtube.com/watch?v=_XF7N6rp9Jw
- Written evidence (RTR0073). (2022). Breast Cancer Now and UK Parliament. <https://committees.parliament.uk/writtenevidence/42740/pdf/>
- Yadav, S.-P., & Yadav, S. (2020). Fusion of medical images in wavelet domain: a hybrid implementation. *Computer Modeling in Engineering & Sciences*, 122(1), 303-321. <https://doi.org/10.32604/cmes.2020.08459>
- Zainudin, Z., Shamsuddin, S. M., & Hasan, S. (2021). Deep layer convolutional neural network (CNN) Architecture for breast cancer classification using histopathological images. In A. E. Hassanien (Ed.), *Machine Learning and Big Data Analytics Paradigms: Analysis, Applications and Challenges* (pp. 347–364). Springer Nature Switzerland. https://doi.org/10.1007/978-3-030-59338-4_18
- Zeiler, M. D., Taylor, G. W., & Fergus, R. (2011). Adaptive deconvolutional networks for mid and high level feature learning. *2011 International Conference on Computer Vision* (pp. 2018–2025). IEEE. <https://doi.org/10.1109/ICCV.2011.6126474>
- Zhang, W. (1990). Parallel distributed processing model with local space-invariant interconnections and its optical architecture. *Applied Optics*, 29(32), 4790–4796. <https://doi.org/10.1364/AO.29.004790>